SIMILARITY CRITERIA FOR "FULL" AND "SCALE" AIRCRAFT ON THE LATERAL STABILTY ANALYSIS

Stefan BOGOS[1], Ion STROE[2]

Acesta lucrare reprezintă un studiu asupra creşterii acurateţii rezultatelor care privesc stabilitatea lateral-directională a unui avion real aflat în stadiul de proiectare, folosind rezultatele obtinute pe un model zburator construit la scară. Sunt propuse criterii coerente privind similitudinea dimensională, masică, inertială şi cinematică între avionul real şi modelul mockup la scară. Rezultatele comparative între avionul real şi modelul la scară arată aceleaşi valori pentru factorul de amortizare în modul „ruliu olandez". Sunt obţinute valori factorizate cu o constanta, pentru caracteristicile de timp în modurile „ruliu olandez", „ruliu" şi „spiral".

This paper aims to achieve a study for increasing the level of confidence in the results concerning the lateral-directional stability of a real aircraft in the design stage, using the results from a flying scale model. Similarity coherent criteria are proposed for the dimensions, mass, inertia and cinematic characteristics between the real aircraft and the scale mockup model. Comparison between the real aircraft and the scale model plane show the same values for the damping factor in "Dutch roll". Values factored with a constant are obtained for the time characteristics in "Dutch roll", "Roll" and "Spiral" modes.

Keywords: Lateral aircraft stabilty, similarity, scale mockup, dutch roll, spiral

Nomenclature

b - span (m); S - wing area(m^2); m -mass (kg); I_x, I_z, I_{xz} -moment of inertia(kgm^2);

V, V_∞ - speed(m/s); $\vec{\omega}(p,q,r)$ - (roll, pitch, yaw speed) (rad/s);

$\hat{p} = pb/2V$, $\hat{r} = rb/2V$ - nondimensional roll, yaw speed (rad);

q - dynamic pressure (N/m^2); α, β - incidence, sideslip angle (rad) ;

$C_{y\beta}, C_{l\beta}, C_{n\beta}$ - side force, roll, yaw derivatives due to sideslip (rad^{-1});

$C_{y\hat{p}}, C_{l\hat{p}}, C_{n\hat{p}}$ - side force, roll, yaw damping derivatives in roll (rad^{-1});

$C_{y\hat{r}}, C_{l\hat{r}}, C_{n\hat{r}}$ -side force, roll, yaw damping derivatives in yaw (rad^{-1});

θ, Φ - pitch, bank angle (rad); $t^* = b/2V$ -nondimensionl time (s);

[1] Eng., INCAS-National Institute for Aerospace Research "Elie Carafoli", Bucharest , bogos@incas.ro

[2] Professor, Department of Mechanics, University POLITECHNICA of Bucharest , ion.stroe@gmail.com

SF - scale factor between Full aircraft and Scale mockup;

$1/SF$ - scale factor between Scale mockup and Full aircraft;

Subscript:

S - is related to the Scale mockup; F - is related to the Full aircraft;

Other notations are self-explanatory or are explained in the paper.

1. Introduction

The Lateral-Directional airplane Stability is of a great importance for the Flying Qualities related to the passenger comfort, in an airliner, or for the fighting capabilities for a military aircraft. The Flying Quality Levels are defined in MIL (Military Specification - Flying Qualities of Piloted Airplanes). The requirement on dynamic stability is typically expressed in terms of the damping and frequency of a natural mode. Thus the USAF (1980) requires the damping and frequency of the lateral oscillation for various flight phases at specific range values, according to the defined quality "Level 1", "Level 2" and "Level 3". Although the FAR (Federal Airworthiness Requirements) do not set specific flying quality levels, common design practice is to adopt the military definitions.

Airplanes must be designed to satisfy the Level 1 flying quality requirements with all systems in their normal operating state. If, for an already built aircraft, after the first flight test program, an unsatisfactory lateral stability is recorded, important and expensive changes have to be done. The following example show that British certification requirements relating to engine-out go-around forced Boeing to increase the height of the tail fin on all 707 variants, as well as to add a ventral fin, which was retrofitted on earlier 120 up to 220 aircraft. The arrangement with additional vertical ventral fins, appear also to other aircraft: Beechcraft 1900 D (with vertical tailets), Jetstream 41, DO 228, Metro 23, TBM 700, F 406, F 16. These modifications also aided in the mitigation of dutch roll by providing more yaw stability. A detailed study about this tendency was pointed in [1]. A "yaw damper" is also a solution to improve the lateral flying qualities.

The lateral-directional stability analysis requests, as input data, aircraft mass, inertia and the detailed aerodynamic coefficients and derivatives. The classical assumptions for the general equations of the unsteady aircraft motion analysis imply: uncoupling "longitudinal" and "lateral", small perturbation and linear equations of the motion. Sometimes, this theoretical hypothesis, together with an uncertainty on the input data, would produce unsatisfactory results for the lateral-directional flying qualities.

To increase the level of confidence for the output results, both wind tunnel tests and specific flight tests are desired. If coherent similarity criteria between "Full aircraft" and "Scale mockup" are respected, the identification of the flying results would be easier to be understood. This paper aims to achieve a study for

increasing the quality of the results concerning the lateral-directional stability of a real aircraft using the results from a flying scale model. The scale ratio of the scale mockup related to the full aircraft was 1/10. The content of this report completes the topics from [2] and details how to translate the recorded lateral-directional stability parameters from the flying mockup to the real aircraft.

2. The aerodynamic model

The following is a short presentation about a specific practical method regarding the evaluation of the pressure distribution on the outside surface of the aircraft. A general steady subsonic motion composed by a translation with $\vec{V}_\infty$ velocity and an aircraft rotation with angular velocity $\vec{\omega}(p,q,r)$ is assumed. Also it is assumed a potential flow, without viscous effects. The "aerodynamics" approaches of the geometry according with "small perturbations" are accepted. The potential theory is used to get the solution. The three-dimensional boundary value problem is solved using the "boundary element method", [7]. The "boundary element" method is a specific method, developed especially for differential equations of Laplace or Poisson type.

The way to solve the potential equation is by using singularities of source type, vortices or doublets in order to form the integral equation that describes the potential. Fig. 1 is a representation of the aerodynamic mesh for the aircraft model, "Full scale" that was used in this present evaluation.

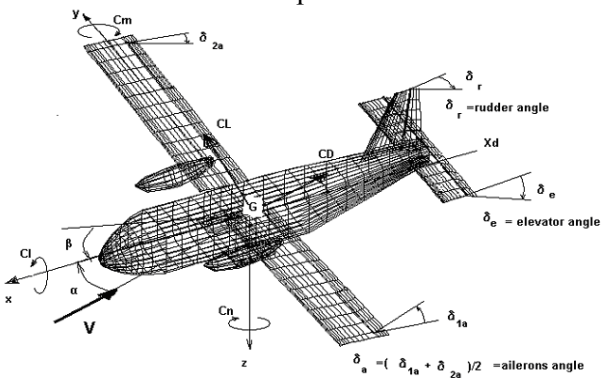

Fig. 1 Aerodynamic mesh, "Full Aircraft"

By using the Green theorem, we obtain that the potential in a point *P*, exterior to the *S* surface of the aircraft, is given by the expression (1):

$$\phi(P) = -\frac{1}{4\pi}\int_S \frac{1}{r(p,q)}\frac{\partial \phi}{\partial n}(q)dS + \frac{1}{4\pi}\int_S \phi(q)\frac{\partial}{\partial n}\left(\frac{1}{r(p,q)}\right)_q dS \qquad (1)$$

The boundary conditions described through equations (2), applied to the disturbance potential φ are as follows:

$$\begin{cases} \Delta\varphi = 0, on\ the\ outside\ S, region \\ \left(\dfrac{\partial\varphi}{\partial n}\right)_S = -\vec{n}\cdot\vec{V}_\infty, \quad on\ the\ body \\ \varphi = 0, \quad at\ \infty \end{cases} \tag{2}$$

Let $\sigma(q)$ be the intensity of a sources panel in a point q on the surface of the non lifting body, or on the skeleton of the wing, and $\Gamma(k)$ the intensity of the circulation of a horseshoe vortex in the point k on the medium surface.

Condition (2) and (1), applied to the specific singularities will give the equation :

$$2\pi\sigma(p) - \int_S \frac{\partial}{\partial n_p}\left(\frac{1}{r(p,q)}\right)\sigma(q)ds + \frac{1}{4\pi}\vec{n}(p)\sum_{k=1}^{Nk}\int_{l_k}\frac{\vec{r}(p,k)\times d\vec{r}}{r^3(p,k)}\Gamma(k) = -\vec{n}(p)\vec{V}_\infty \tag{3}$$

In equation (3), $\vec{n}(p)$ is the "exterior normal" vector to the surface S in the point p, with l_k identifying the semi infinite horseshoe vortex.

It is a contribution that the direction of every free vortex is the same with the local undisturbed velocity, $\vec{V}_{\infty i}$, composed from translation and rotation, as in the relation (4):

$$\vec{V}_{\infty i} = \vec{V}_\infty + \vec{\omega}\times\vec{r}_i \tag{4}$$

where $\vec{r}_i$ is the local position vector.

The numerical resolution of the second kind Fredholm integral equation (3) relies on the approximation of integrals as follows:

$$2\pi\sigma_i(p) - \sum_{j=1}^{Nq}\sigma_j(q)\int_{S_j}\frac{\partial}{\partial n_i(p)}\left(\frac{1}{r(p,q)}\right)ds + \frac{1}{4\pi}\vec{n}_i(p)\sum_{k=1}^{Nk}\Gamma(k)\int_{l_k}\frac{\vec{r}(p,k)\times d\vec{r}}{r^3(p,k)} = -\vec{n}_i\vec{V}_{\infty i} \tag{5}$$

The following notations (6) present the induced velocity by a unitary sources panel from point j or by a vortex horseshoe from point k in a collocation point i from the aircraft surface.

$$a_{ij} = \int_{S_j}\frac{\partial}{\partial n_{i(p)}}\left(\frac{1}{r(p,q)}\right)ds, \quad a_{ik} = \frac{1}{4\pi}\vec{n}_i(p)\int_{l_k}\frac{\vec{r}(p,k)\times d\vec{r}}{r(p,k)^3} \tag{6}$$

The relations (5) and (6) will give a linear algebraic equations system for the unknown σ_j and Γ_k, that are written formal in (7) as x_j.

$$\sum_{j=1}^{n} a_{i,j}x_j = b_i \quad , i = 1,n \tag{7}$$

A robust iterative (Conjugate Gradient) solver is used for the large full matrix from (7). The results of the numerical simulations lead to the pressure coefficients and finally, by integration, to the aerodynamic coefficients and derivatives. The method was implemented “in-house” for a FORTRAN software code: AEROLOADS.

3. Results for the lateral derivatives

The lateral derivatives that were used for lateral-directional stability were evaluated using wind tunnel testing results [3] and numerical data.

The following relations (8) give the analytical expressions for the nondimensional aerodynamic lateral derivatives.

$$\begin{aligned} C_{y\beta}(C_L) &= -0.945 + 0.178\, C_L \\ C_{n\beta}(C_L) &= 0.101 + 0.0129\, C_L - 0.0181\, C_L{}^2 \\ C_{l\beta}(C_L) &= -0.155 + 0.106\, C_L \end{aligned} \tag{8}$$

The relations (8) pointed out the variation of the lateral derivatives with the lift coefficient C_L. This type of dependence is due to the interference between the wings, rear fuselage with the vertical tail. This type of behaviour is pointed out also in [4], [8], [9] and [10].

4. Results for the rotary damping derivatives

In the first aircraft design stage, the rotary damping derivatives are estimated with closed analytical formulae or using diagrams [4], [7] and [10]. This kind of approach might give some inconsistency due to the specific shape of the aircraft and the local interference. So, the numerical simulation was used to evaluate the rotary damping derivatives. The aerodynamic model is shown in the fig. 1. There were calculated the variation of the nondimensional rotary derivatives with the lift coefficient, C_L in the range for which the aerodynamic phenomena are linear.

The numerical results were processed to get some analytical formulae that are useful for stability analysis of the aircraft. The relations (9) present these data related to the nondimensional rotary speeds: $\hat{p}$, $\hat{r}$.

$$
\begin{aligned}
&C_{y\hat{p}}(C_L) = -0.117 + 0.145\,C_L \\
&C_{l\hat{p}}(C_L) = -0.607 - 0.01\,C_L \\
&C_{n\hat{p}}(C_L) = -0.0056 - 0.0434\,C_L \\
&C_{y\hat{r}}(C_L) = 0.256 + 0.048\,C_L \\
&C_{l\hat{r}}(C_L) = 0.082 + 0.175\,C_L \\
&C_{n\hat{r}}(C_L) = -0.116 - 0.091\,C_L
\end{aligned}
\tag{9}
$$

5. Aircraft Lateral-Directional analysis motion

The present analysis uses the dimensional small disturbance equations system for the lateral directional motion, [5], [6], given through the linearization of the general equations. It was made the assumption that the motion of the airplane consists of small deviations from a reference steady flight condition. The initial conditions are: for incidence α_0, pitch attitude θ_0 and speed V. The controls aileron and rudder are kept in the fixed positions.

The formal lateral-directional dynamic system is (10):

$$\dot{\boldsymbol{x}} = \boldsymbol{A}\boldsymbol{x} \tag{10}$$

Hence $\boldsymbol{x}$ is the state vector and $\boldsymbol{A}$ is the system matrix, respectively:

$$\boldsymbol{x} = \left[\beta\ p\ r\ \Phi\right]^T \tag{11}$$

The matrices of the aircraft lateral model are defined in equation (12), based on [6]. The formal form (12) is related to the aircraft body axis reference system.

$$
\boldsymbol{A} = \begin{bmatrix}
\dfrac{Y_\beta}{mV} & \dfrac{Y_p}{mV} + \sin\alpha_0 & \dfrac{Y_r}{mV} - \cos\alpha_0 & \dfrac{g}{V}\cos\theta_0 \\
\dfrac{I_z L_\beta + I_{xz} N_\beta}{I_x I_z - I_{xz}^2} & \dfrac{I_z L_p + I_{xz} N_p}{I_x I_z - I_{xz}^2} & \dfrac{I_z L_r + I_{xz} N_r}{I_x I_z - I_{xz}^2} & 0 \\
\dfrac{I_x N_\beta + I_{xz} L_\beta}{I_x I_z - I_{xz}^2} & \dfrac{I_x N_p + I_{xz} L_p}{I_x I_z - I_{xz}^2} & \dfrac{I_x N_r + I_{xz} L_r}{I_x I_z - I_{xz}^2} & 0 \\
0 & 1 & \tan\theta_0 & 0
\end{bmatrix}
\tag{12}
$$

Usually, the roots of the characteristic equation $\left|\lambda\boldsymbol{I} - \boldsymbol{A}\right| = 0$ give the eigenvalues: a conjugate complex pair $\lambda_{1,2D}$ and two real roots λ_{3R} and λ_{4S} in algebraic form (13):

$$
\begin{aligned}
&\lambda_{1,2D} = n \pm i\omega \\
&\lambda_{3R} = n_R \\
&\lambda_{4S} = n_S
\end{aligned}
\tag{13}
$$

The complex eigenvalues correspond to Dutch roll, a damped oscillatory motion with low frequency (14):

$$\lambda_{1,2D} = -\varsigma_D \omega_n \pm \mathrm{i}\omega_n \sqrt{1-\varsigma_D{}^2}$$
$$with \quad \omega_n = \sqrt{n^2+\omega^2}\ , \quad \varsigma_D = -\frac{n}{\omega_n} \tag{14}$$

where ζ_D, ω_n are the Dutch roll damping ratio and the undamped natural circular frequency. The real root λ_R representing a fast convergent motion is the Roll mode and λ_S is the Spiral mode that may be a convergent or slightly divergent.

6. Similarity criteria and aerodynamic equivalence: Full and Scale

It can be seen that the coefficients from the lateral state matrices $\boldsymbol{A}$ from (12) are function of the aircraft dimensions, inertia properties and the stability derivatives. Also the initial conditions imply a definition for aircraft velocity, V.

Similarity coherent criteria are proposed for the dimensional and inertial characteristics between a real aircraft and the scale flying mockup model.

It is assumed that the linear scale factor SF is 10. The table 1 presents some relations related to a comparative analysis between "Full aircraft" and "Scale mockup".

Table 1

Similarity criteria between "Full Aircraft" and "Scale flying Mockup"

Criteria	$(Full)_F$ Aircraft	$(Scale)_S$ Mockup	Similarity Ratio: Scale/Full	Similarity ($SF = 10$)
Linear (e.g. span)	21.64 m	2.164 m	$1/SF$	1/10
Area (e.g. wing)	42.92m^2	0.429m^2	$1/SF^2$	1/100
Volume (fuselage)	28 m^3	0.028 m^3	$1/SF^3$	1/1000
Mass (MTOW)	8400 kg	8.4 kg	$1/SF^3$	1/1000
Inertia (e.g. I_x)	130117 kgm^2	1.301 kgm^2	$1/SF^5$	1/100000
Controls deflection	The same		1	1
Thrust (maxim)	3400 kgf	1.4…3.4 kgf	$1/SF^3$	1/1000

The similarity for the inertia properties may be resolved with a specific mass distribution inside the model, assuming also similarity for weight. Figure 2 presents a solution to control inertia/mass properties with some internal auxiliary blocks distribution.

Fig 2. Scale mockup with internal blocks distribution for inertia simulation

The following relations detail the dimensional form of the stability derivatives.

$$Y_\beta = qSC_{y\beta}(C_L), \qquad L_\beta = qSbC_{l\beta}(C_L), \qquad N_\beta = qSbC_{n\beta}(C_L) \tag{15}$$

$$Y_p = qSC_{y\hat{p}}(C_L)\left(\frac{b}{2V}\right), L_p = qSbC_{l\hat{p}}(C_L)\left(\frac{b}{2V}\right), N_p = qSbC_{n\hat{p}}(C_L)\left(\frac{b}{2V}\right) \tag{16}$$

$$Y_r = qSC_{y\hat{r}}(C_L)\left(\frac{b}{2V}\right), L_r = qSbC_{l\hat{r}}(C_L)\left(\frac{b}{2V}\right), \quad N_r = qSbC_{n\hat{r}}(C_L)\left(\frac{b}{2V}\right) \tag{17}$$

It can be seen that these stability derivatives are dependent on the lift coefficient C_L through the nondimensional aerodynamic derivatives from (8) and (9).

For a coherent comparative analysis it is proposed that the lateral and rotary aerodynamic derivatives for Full scale aircraft and Scale flying mockup are the same. This assumption will imply that the lift coefficient for Full model C_{LF}, is equal to the lift coefficient for Scale model C_{LS}:

$$C_{LF} = C_{LS} \tag{18}$$

The following relations detail the form for the lift coefficients C_{LF} and C_{LS},

$$C_{LF} = \frac{2m_F g}{\rho S_F {V_F}^2}, C_{LS} = \frac{2m_S g}{\rho S_S {V_S}^2} \tag{19}$$

Using the similarity criteria from table (1) and the relation (18), one obtains the Scale flying mockup velocity V_S, in the form (20):

$$V_S = \sqrt{\frac{1}{SF}} \cdot V_F \tag{20}$$

where SF is the linear scale factor between Full model and Scale model.

The equivalents for the aerodynamic derivatives for the real aircraft and the scale mockup, are achieved by choosing a flight regime (20) that preserves the

lift coefficient C_L. It is assumed that Reynolds effects are of secondary importance related to the lateral and damping derivatives.

7. Lateral modes, "Full aircraft " and "Scale mockup" comparison

Computations were performed for the following numerical values presented in the table 2.

Table 2

Input data for numerical simulation

	$(Full)_F$ aircraft	$(Scale)_S$ mockup	SIMILARITY ($SF = 10$)
Span; b (m)	21.64	2.164	$1/SF$
Wing area; S (m^2)	42.92	0.429	$1/SF^2$
Mass ; m (kg)	8400	8.4	$1/SF^3$
Inertia ; I_x, I_z, I_{xz} ($kg\ m^2$)	130117, 162962, 4384	1.301, 1.629, 0.0438	$1/SF^5$
Speed (m/s)	102	32.25	$\sqrt{\frac{1}{SF}}$
Lift Coefficient C_L	0.3	0.3	1
Lateral aerodynamic derivatives (8)	The same		1
Lateral rotary derivatives (9)	The same		1

A numerical integration method, Runke-Kutta of 4-th order from Mathcad was used to evaluate the solution of the system (10), both for Full aircraft and Scale mockup. The eigenvalues and eigenvectors were processed.

The steady straight flight level with an incidence $\alpha_0 = -0.0139\ rad$ is the reference condition.

The initial conditions for the state variable $\boldsymbol{x}_0$ assume lateral sharp gusts that imply a perturbation for sideslip β as is given in (21).

$$\boldsymbol{x}_0 = [0.1, 0, 0, 0]^{\boldsymbol{T}} \tag{21}$$

The state matrices $\boldsymbol{A_S}$ for Scale mockup and $\boldsymbol{A_F}$ for Full aircraft are given respectively in (23) and (24):

$$\boldsymbol{A_S} = \begin{bmatrix} -0.8998 & -0.0164 & -0.9907 & 0.3041 \\ -54.7660 & -9.3243 & 2.0066 & 0.0000 \\ 36.0238 & -0.4784 & -1.4599 & 0.0000 \\ 0.0000 & 1.0000 & -0.0139 & 0.0000 \end{bmatrix} \tag{23}$$

$$\boldsymbol{A_F} = \begin{bmatrix} -0.2845 & -0.0164 & -0.9907 & 0.0962 \\ -5.4766 & -2.9486 & 0.6345 & 0.0000 \\ 3.6024 & -0.1513 & -0.4617 & 0.0000 \\ 0.0000 & 1.0000 & -0.0139 & 0.0000 \end{bmatrix} \tag{24}$$

The eigenvalues λ_S for Scale mockup and λ_F for Full aircraft become:

$$\boldsymbol{\lambda_S} = \begin{bmatrix} -0.9790 + 6.2426i \\ -0.9790 - 6.2426i \\ -9.7162 \\ -0.0100 \end{bmatrix} \text{ and } \boldsymbol{\lambda_F} = \begin{bmatrix} -0.3096 + 1.9741i \\ -0.3096 - 1.9741i \\ -3.0725 \\ -0.0032 \end{bmatrix} \tag{25}$$

All three modes are seen to be stable. The first is a damped oscillation, Dutch Roll. The other two are aperiodic convergent: one very rapid, Roll mode, and one very slow, Spiral mode.

Due to the similarity and the aerodynamic equivalence, relation (25) shows dependence of the eigenvalues $\boldsymbol{\lambda_F}$ and $\boldsymbol{\lambda_S}$ as follows:

$$\lambda_S = \sqrt{SF}\,\lambda_F \quad or \quad \lambda_S = \sqrt{10}\,\lambda_F \tag{26}$$

The above similarity criteria become an invariant for the eigenvalues if the lateral-directional analysis is made using NACA Nondimensional System [4]. Using this technique one obtains the same eigenvalues λ_S and λ_F.

In this case the nondimensional time constants t_F^* for Full aircraft and t_S^* for Scale mockup are in a relation similar to (26):

$$t_F^* = \sqrt{SF}\,t_S^* \quad or \quad t_F^* = \sqrt{10}\,t_S^* \tag{27}$$

The aircraft flying qualities are evaluated using the following time characteristics:

$$\begin{aligned} &Period: \quad T = \frac{2\pi}{\omega} = \frac{2\pi}{\omega_n\sqrt{1-\varsigma^2}} \\ &Time\ to\ half\ or\ double: t_{half,double} = \frac{0.693}{|n|} = \frac{0.693}{|\varsigma|\omega_n} \\ &Cycles\ to\ half\ or\ double: N_{half,double} = \frac{0.11\omega}{|n|} = \frac{0.11\sqrt{1-\varsigma^2}}{|\varsigma|} \\ &Time\ constant: \quad \tau_{R,S} = -\frac{1}{n_{R,S}} \end{aligned} \tag{28}$$

Table 3 shows a comparison for the characteristics times and damping ratio of the Full aircraft and Scale mockup.

Table 3

Characteristics Times-Lateral Modes

M O D E		$(Scale)_S$ mockup	$(Full)_F$ aircraft	SIMILARITY $(SF = 10)$
Dutch Roll (damped oscillation)	ξ	0.155	0.155	$\xi_F = \xi_S$
	ω_n	6.139	1.998	$\omega_{nF} = \omega_{nS} / \sqrt{SF}$
	T	1.01	3.183	$T_F = T_S \sqrt{SF}$
	t_{half}	0.708	2.239	$t_{half_F} = t_{half_S} \sqrt{SF}$
	N_{half}	0.701	0.701	$N_{half_F} = N_{half_S}$
Roll (convergent)	τ	0.103	0.326	$\tau_F = \tau_S \sqrt{SF}$
	t_{half}	0.07	0.226	$t_{half_F} = t_{half_S} \sqrt{SF}$
Spiral (convergent)	τ	100.35	317.336	$\tau_F = \tau_S \sqrt{SF}$
	t_{half}	69.558	219.96	$t_{half_F} = t_{half_S} \sqrt{SF}$

The results from table 3 show the same damping ratio and cycles in Dutch Roll. The time characteristics for the Full aircraft are obtained from those of the Scale mockup multiplied with a constant, $\sqrt{SF}$.

The transient behaviour of the state variables in the lateral-directional motion is displayed respectively in figure 3 for Dutch Roll, figure 4 for Roll mode and figure 5 for Spiral mode.

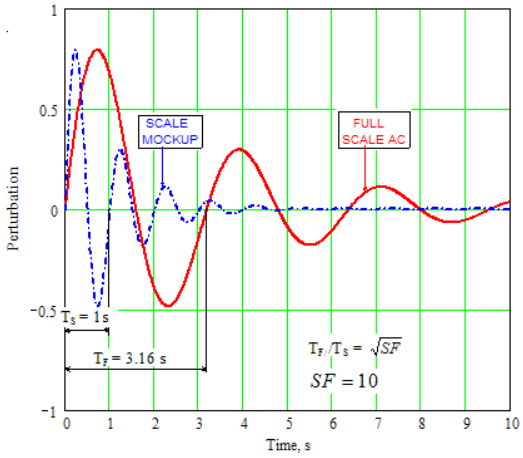

Fig. 3. Characteristics transient, Dutch Roll

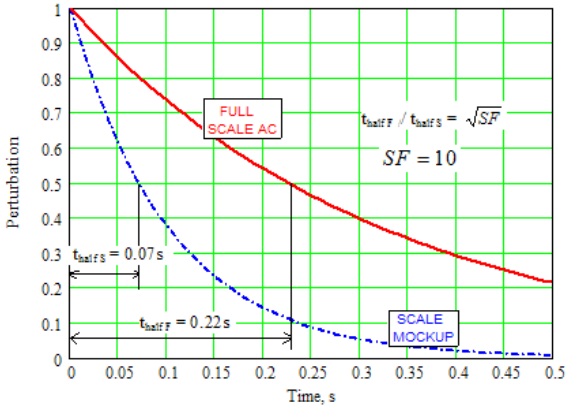

Fig. 4. Characteristics transient, Roll mode

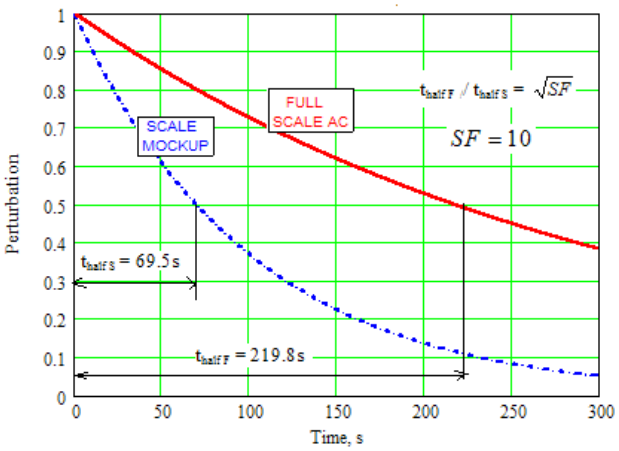

Fig. 5. Characteristics transient, Spiral mode

The aircraft response to a lateral sharp gust from the right side is displayed in the following figures: sideslip response in figure 5, roll response in figure 6, yaw response in figure 7 and bank response in figure 8.

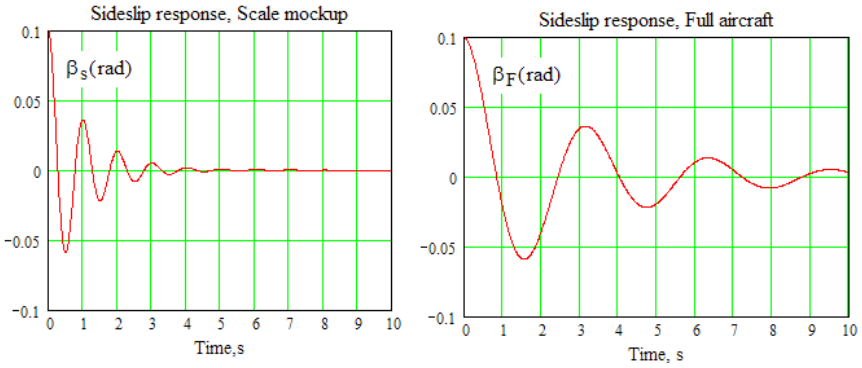

Fig. 6. Sideslip response at a lateral sharp gust, comparison

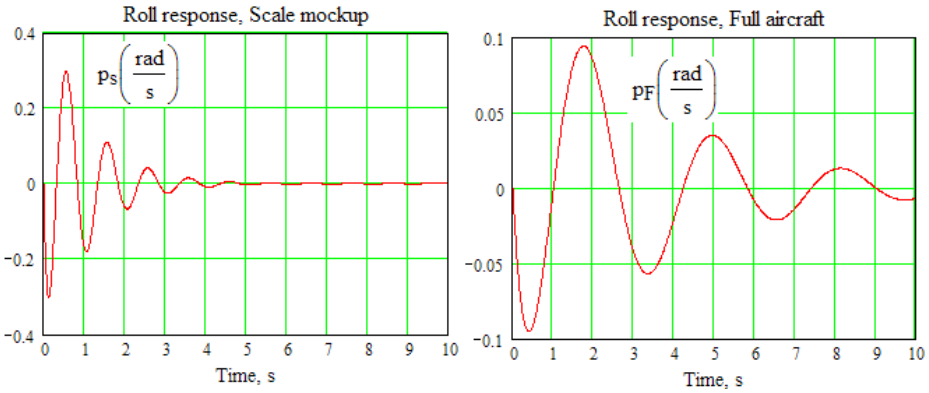

Fig. 7. Roll response at a lateral sharp gust, comparison

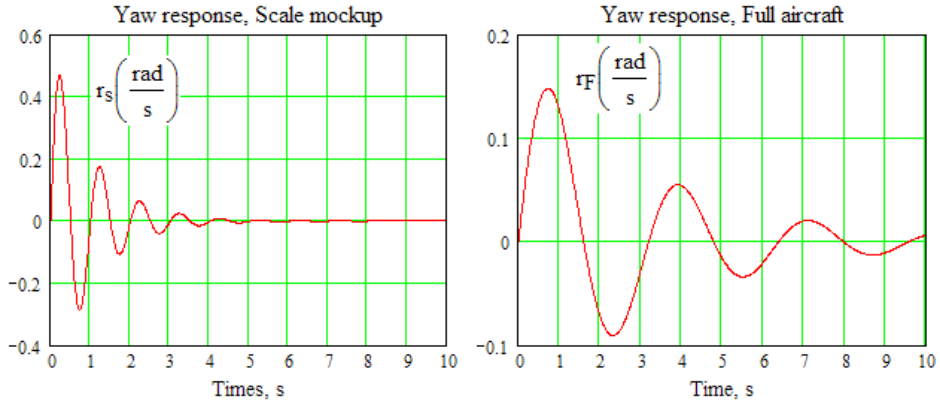

Fig. 8. Yaw response at a lateral sharp gust, comparison

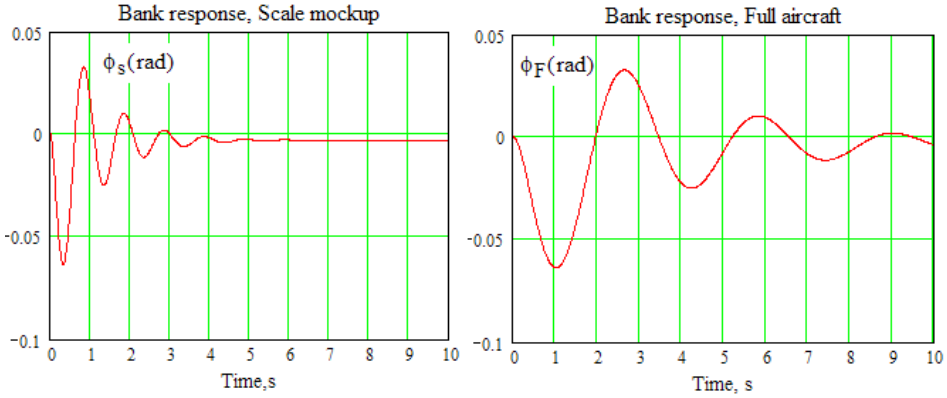

Fig. 9. Bank angle response at a lateral sharp gust, comparison

The comparison between Full aircraft and Scale mockup periods, T, of the damped oscillations shows a relationship as :

$$T_F = T_S\sqrt{SF}, \quad T_F = T_S\sqrt{10} \tag{29}$$

8. Conclusion

This specific analysis about lateral-directional aircraft stability details how to translate, in a coherent mode, the results from a “scale flying mockup” to the “full aircraft”.

A practical “in-house” aerodynamic “boundary element” model was developed and used to evaluate the lateral aerodynamic coefficients and their stability derivatives. These results were completed with available.specific wind tunnel data.

Similarity coherent criteria for the dimensional, inertial and mass characteristics between the real aircraft and the scale mockup model are proposed.

The equivalents for the aerodynamic derivatives for the real aircraft and the scale mockup, are achieved by choosing a flight regime that preserves the lift coefficient.

Comparison between the real aircraft and the scale model plane show the same values for the damping factor in "Dutch roll". Factored values with a constant are obtained for the time characteristics in "Dutch roll", “Roll” and “Spiral” modes.

R E F E R E N C E S

[1] *S. Bogos, D. Turcanu*, The Aerodynamic and Dynamic Ventral Fins Effects on a Jet Trainer, 22nd Congress of International Council of the Aeronautical Sciences, Harrogate, UK, 2000, Paper ICAS 2000-2.1.4

[2] *Brad A. Seanor,* Flight Testing of a Remotely Piloted Vehicle for Aircraft Parameter Estimation Purposes, Dissertation for the degree of PhD in Aerospace Engineering, Morgantown, West Virginia, 2002

[3] *INCAS-Bucharest,* Wind Tunnel Test Program, Contract 1464/2006

[4] *Etkin B*. Dynamics of Flight-Stability and Control. John Wiley & Sons, NY, 1959

[5] *Etkin B*. Dynamics of Atmospheric Flight, John Wiley & Sons , NY, 1972

[6] *Etkin B., Reid L. D*., Dynamics of Flight-Stability and Control, Third Edition, John Wiley & Sons, NY, 1996

[7] *Hess J. L., Smith A. M. O.,* Calculation of Potential Flow about arbitrary bodies, Progress in Aeronautical Sciences, Vol. 8, 1967

[8] *Perkins C. D.,Hage R. E.,* Airplane Performance Stability and Control, John Wiley & Sons, NY, 1967

[9] *Lan C. T., Roskam J.,* Airplane Aerodynamics and Performance, DAR Corporation, 2003

[10] *Roskam J.,* Airplane Flight Dynamics and Automatic Flight Controls, Part I and II, DAR Corporation, 2003